



# Regional differences in raindrop size distribution observed from disdrometers in South Korea and their possible causes

Joohyun Lee<sup>1</sup> · Han-Gyul Jin<sup>1</sup> · Jong-Jin Baik<sup>1</sup>

Received: 20 June 2022 / Accepted: 27 August 2022 / Published online: 9 September 2022  
© The Author(s), under exclusive licence to Springer-Verlag GmbH Austria, part of Springer Nature 2022

## Abstract

In this study, we examine the regional differences in the characteristics of raindrop size distribution (RSD) among three cities (Seoul, Chuncheon, and Jincheon) in South Korea using disdrometer data for the period from 25 July 2018 to 31 July 2021 and investigate possible causes for the differences. Jincheon, the least populated and southernmost city among the three cities, is characterized by the smallest mean rainfall intensity and a relatively high frequency of light rain. These precipitation characteristics are related to the mass-weighted mean diameter  $D_m$  that is smallest and the logarithm of generalized intercept parameter  $\log_{10}N_w$  that is largest in this city. In contrast, Chuncheon, a medium-sized city located in a basin, is characterized by the largest mean rainfall intensity and a relatively high frequency of heavy rain, which is related to the largest  $D_m$  and smallest  $\log_{10}N_w$ . Relatively small (large) convective available potential energy, low (high) cloud top, and high (low) cloud base in Jincheon (Chuncheon) can be responsible for the contrasts in RSD characteristics between the two cities. Seoul, the most populated city, is characterized by the intermediate mean rainfall intensity related to the intermediate  $D_m$  and  $\log_{10}N_w$  between those in Jincheon and Chuncheon. Seoul exhibits the most frequent occurrence of extreme rainfall events and relatively large  $D_m$  for very heavy rain, which can be associated with the most frequent occurrence of large convective available potential energy.

## 1 Introduction

The measurement and analysis of raindrop size distribution (RSD) are important part of cloud physics, and extensive studies have been performed to characterize RSD using disdrometer observations in many regions of the world (Nzeukou et al. 2004; Leinonen et al. 2012; Giangrande et al. 2014; Murata et al. 2020; Zea et al. 2021). Characterizing RSD can greatly help to improve our understanding of cloud and precipitation processes, estimate rainfall, and parameterize cloud microphysical processes in numerical models.

Many studies have shown that there is strong regional variability in RSD characteristics (Bringi et al. 2003; Seela et al. 2017; Dolan et al. 2018). Bringi et al. (2003) collected disdrometer and radar data from regions of various climate regimes, that is, near equator, tropics, subtropics, continental, oceanic, and High Plains, and classified the data into

stratiform and convective rain using the rain rate and its standard deviation. The RSD data in each of the regions constitutes a cluster in the RSD-parameter space, which results in the identification of three distinct clusters (stratiform rain, maritime-like convective rain, and continental-like convective rain). Dolan et al. (2018) collected disdrometer data from three latitude bands (lower than  $23^\circ$ ,  $23^\circ\text{--}45^\circ$ , and higher than  $45^\circ$  in both hemispheres) and performed the principal component analysis. They identified six groups in the space of the logarithm of generalized intercept parameter and the median volume diameter and showed that each group is associated with specific cloud microphysical processes and that the process which is responsible for the RSD depends on the latitude band. Seela et al. (2017) compared the characteristics in RSD between two islands in western Pacific (Palau and Taiwan). The mass-weighted mean diameter (generalized intercept parameter) is larger (smaller) in Taiwan than in Palau. They suggested that this is linked to the relatively strong convective activity, high storm height, high bright band, and high aerosol concentration in Taiwan.

The regional variability in RSD characteristics has been examined also for smaller spatial scales (Loh et al. 2019; Han et al. 2021; Suh et al. 2021). Han et al. (2021) investigated

✉ Han-Gyul Jin  
hgjin@snu.ac.kr

<sup>1</sup> School of Earth and Environmental Sciences, Seoul National University, Seoul 08826, South Korea

the regional variability of summertime RSD obtained from ten disdrometers in Beijing. The minimum mass-weighted mean diameter and maximum generalized intercept parameter appear in the city center. They speculated that this is related to the urban heat island and aerosol effects. South Korea, located in a peninsula with complex geographical features, shows a regional variability of RSD characteristics within the country. Loh et al. (2019) compared the RSD characteristics between two sites, one in the central region and the other in the southeastern region of South Korea, and showed that the site in the central region tends to receive a relatively large number of small-sized raindrops. Suh et al. (2021) examined how the RSD characteristics change from coastal areas to inland areas in the southern region of South Korea and showed that the coastal areas exhibit multimodal distributions of probability density functions of the mass-weighted mean diameter and logarithm of generalized intercept parameter for stratiform rain while the inland areas do not. They also showed that for convective rain, the RSD parameters have linear relationships with the distance from the coastline.

The studies on disdrometer observation in South Korea have been limited to the southern and central parts of South Korea (Lim et al. 2015; You and Lee 2015; Suh et al. 2016, 2021; Bang et al. 2017; Kim et al. 2019; Loh et al. 2019). Although there is a study in the northwestern part of South Korea (Jwa et al. 2021), about 1 year of observational period in that study is rather short. This study uses the disdrometer data observed for about 3 years at Seoul, Chuncheon, and Jincheon, which are at the northwestern, northern, and central parts of South Korea, respectively. From this study, it can be expected to reveal the RSD characteristics of northern part in South Korea. In addition, the direct comparison between Seoul, which is the largest metropolis in South Korea, and other sites will be of great help in understanding how the RSD characteristics of urban areas with different sizes differ.

In this study, we examine the regional differences in RSD characteristics among three different sites in South Korea using disdrometer data and investigate possible causes for the differences. In Sect. 2, the data and methodology are given. In Sect. 3, the precipitation and RSD characteristics of each of the three sites are characterized and compared. Also, the regional differences in thermodynamic and cloud characteristics that may cause the regional differences in RSD characteristics are investigated. A summary and conclusions are given in Sect. 4.

## 2 Data and methodology

### 2.1 Disdrometer data and RSD parameters

In this study, data from Parsivel<sup>2</sup> disdrometers (Tokay et al. 2014) installed at three different sites (Seoul, Chuncheon,

and Jincheon) in South Korea are used to investigate the regional variations in RSD parameters. Figure 1 shows the geographical locations of the disdrometers. Seoul is the most populated city in South Korea and manifests the most urban characteristics among the three sites. Chuncheon is a medium-sized city that is located in a basin and most distant from the coast and thus highly likely to have the continental and orographic characteristics among the three sites. Jincheon is a small city and located at the southernmost latitude among the three cities. The elevations of the three disdrometer sites are similar to each other, which are 142, 136, and 138 m for Seoul, Chuncheon, and Jincheon, respectively.

The Parsivel<sup>2</sup> disdrometer is an optical disdrometer having a transmitter and a receiver of a laser beam of 650-nm wavelength. The sampling volume between them is 5400 mm<sup>3</sup> (180 mm × 30 mm × 1 mm). When a precipitating particle falls through the sampling volume, the diameter and fall velocity of the particle are determined by the maximum reduced voltage and the signal duration, respectively. The determined diameter and fall velocity are classified into 32 × 32 non-uniform bins. The range of particle diameter is 0–26 mm with 32 bins, but the first two bins are not considered due to the low signal-to-noise ratio. For liquid precipitation, which is the main concern of this study, the range is confined to 0.25–8 mm. The range of fall velocity is 0–22.4 m s<sup>-1</sup> with 32 bins. The sampling interval is 1 min.

Optical disdrometers measure drop size and fall velocity without influencing drop behavior during measurement, significantly reducing measurement errors from drop breakup and splattering, which is a great advantage over impact disdrometers (Kathiravelu et al. 2016). However, there still exist several known measurement error sources for the Parsivel<sup>2</sup> disdrometer, such as the effects of strong winds, drops partially passing through the sampling volume, drops splashing on impact with the instrument, multiple drops simultaneously passing through the sampling volume (Angulo-Martínez et al. 2018). Concerning these error sources, the data of drops that fall too fast or too slowly for their sizes (drops with fall velocities 60% larger than or 60% smaller than those from the fall velocity–diameter relationship of Atlas et al. (1973)) are excluded, which is similar to the quality control method of Jaffrain and Berne (2011). In addition, following Thompson et al. (2015), the 1-min disdrometer data with rain rate smaller than 0.05 mm h<sup>-1</sup> or with total drop counts less than 100 are excluded, and the remaining data are used for analysis if they exist consecutively for 3 or more minutes.

The observational period is about 3 years from 25 July 2018 to 31 July 2021. The dates when data from any of the three sites are missing are excluded. As a result, the number of 1-min disdrometer data is 53,340 for Seoul, 52,787 for Chuncheon, and 65,405 for Jincheon.

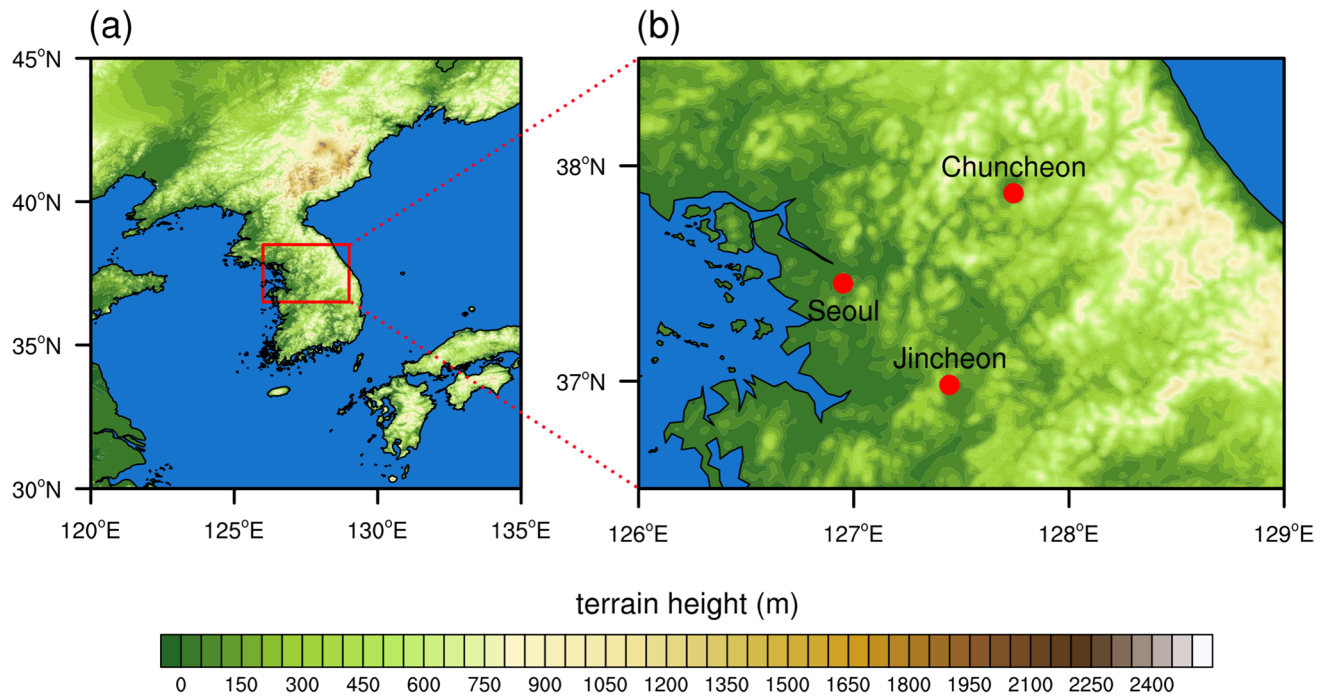


**Fig. 1** **a** Topographic map of South Korea and its surrounding regions and **b** zoomed area with locations of the three disdrometers (red circles)

Each 1-min disdrometer data has the information of the number of raindrops in each diameter and fall velocity bin. From the data, the number concentration of raindrops per unit volume per unit size interval in the  $i$ th diameter bin  $N(D_i)$  ( $\text{m}^{-3} \text{ mm}^{-1}$ ) is calculated as

$$N(D_i) = \sum_{j=1}^{32} \frac{n_{ij}}{A_i V_j \Delta t \Delta D_i} \quad (1)$$

where  $n_{ij}$  is the number of raindrops in the  $i$ th diameter and  $j$ th fall velocity bin,  $A_i$  ( $\text{m}^2$ ) is the effective sampling area for the  $i$ th diameter bin,  $V_j$  ( $\text{m s}^{-1}$ ) is the fall velocity for the  $j$ th fall velocity bin,  $\Delta t$  (s) is the sampling interval, and  $\Delta D_i$  (mm) is the size interval of the  $i$ th diameter bin (here,  $D_i$  is the mid-value of the  $i$ th diameter bin).

Many RSD parameters can be calculated using  $N(D_i)$ . The  $n$ th-order moment of RSD  $M_n$  is defined by

$$M_n = \int D^n N(D) dD \quad (2)$$

For the disdrometer data, Eq. (2) is rewritten as

$$M_n = \sum_{i=3}^{23} D_i^n N(D_i) \Delta D_i \quad (3)$$

The first two bins ( $i=1, 2$ ) and last nine bins ( $i=24-32$ ) are not considered due to the low signal-to-noise ratio and

the consideration of liquid precipitation only, respectively. The total number concentration  $N_t$  ( $\text{m}^{-3}$ ), rainwater content  $W$  ( $\text{g m}^{-3}$ ), and radar reflectivity  $Z$  ( $\text{mm}^6 \text{ mm}^{-3}$ ) are expressed using the moments of RSD as

$$N_t = M_0 \quad (4)$$

$$W = \frac{10^{-3} \pi}{6} \rho_w M_3 \quad (5)$$

$$Z = M_6 \quad (6)$$

where  $\rho_w$  ( $\text{g cm}^{-3}$ ) is the liquid water density. The rain rate  $R$  ( $\text{mm h}^{-1}$ ) is expressed by

$$R = 6\pi \times 10^{-4} \sum_{i=3}^{23} \sum_{j=1}^{32} D_i^3 \frac{n_{ij}}{A_i \Delta t} \quad (7)$$

Here, to see the contribution of the rain rate for each diameter bin to the total rain rate, the rain rate for the  $i$ th diameter bin  $R(D_i)$  ( $\text{mm h}^{-1} \text{ mm}^{-1}$ ) (Ma et al. 2019) is calculated by

$$R(D_i) = 6\pi \times 10^{-4} \sum_{j=1}^{32} D_i^3 \frac{n_{ij}}{A_i \Delta t \Delta D_i} \quad (8)$$

which satisfies

$$R = \sum_{i=3}^{23} R(D_i) \Delta D_i \quad (9)$$

The 1-min disdrometer data can be described by the normalized gamma drop size distribution (Testud et al. 2001) as

$$N(D) = N_w \frac{(4 + \mu)^{4+\mu}}{4^4} \frac{\Gamma(4)}{\Gamma(4 + \mu)} \left( \frac{D}{D_m} \right)^\mu \exp \left[ -(4 + \mu) \frac{D}{D_m} \right] \quad (10)$$

where  $\mu$  is the shape parameter of the gamma drop size distribution,  $N_w$  ( $\text{m}^{-3} \text{ mm}^{-1}$ ) is the generalized intercept parameter,  $D_m$  (mm) is the mass-weighted mean diameter, and  $\Gamma$  is the gamma function.  $N_w$  and  $D_m$  are given by

$$N_w = \frac{4^4}{\pi \rho_w} \left( \frac{10^3 W}{D_m^4} \right) \quad (11)$$

$$D_m = \frac{M_4}{M_3} \quad (12)$$

The 1-min disdrometer data can also be described by the gamma drop size distribution in the following form (Ulbrich 1983; Cao and Zhang 2009):

$$N(D) = N_0 D^\mu \exp(-\Lambda D) \quad (13)$$

where  $N_0$  ( $\text{m}^{-3} \text{ mm}^{-1-\mu}$ ) is the intercept parameter and  $\Lambda$  ( $\text{mm}^{-1}$ ) is the slope parameter. The three parameters are calculated by

$$N_0 = \frac{M_2 \Lambda^{\mu+3}}{\Gamma(\mu + 3)} \quad (14)$$

$$\Lambda = \left[ \frac{M_2}{M_4} (\mu + 3)(\mu + 4) \right]^{\frac{1}{2}} \quad (15)$$

$$\mu = \frac{(7 - 11\eta) - (\eta^2 + 14\eta + 1)^{1/2}}{2(\eta - 1)} \quad (16)$$

where  $\eta$  is given by

$$\eta = \frac{M_4^2}{M_2 M_6} \quad (17)$$

To validate the disdrometer data, the hourly accumulated rainfall amount observed by the disdrometer at each site is compared to that observed by the collocated rain gauge (Fig. 2). Note that for Chuncheon, the comparison is done for the period from 2 October 2019, not for the whole period, because of the poor

data quality before that. At all sites, the disdrometers generally underestimate the hourly accumulated rainfall amount. This underestimation could be caused by the quality control that excludes data that do not satisfy certain conditions. Despite the underestimation, the hourly accumulated rainfall amount from the disdrometer is highly correlated with that from the rain gauge ( $R \geq 0.98$  for all sites), suggesting that the RSD parameters estimated from the disdrometer data have sufficient reliability.

## 2.2 Rain-type classification

Many RSD studies showed that RSD characteristics differ depending on the rain type (Tokay and Short 1996; Bringi et al. 2003; Niu et al. 2010; Chen et al. 2017; Seela et al. 2017; Jwa et al. 2021). To determine the rain type of each 1-min disdrometer data, the method suggested by Bringi et al. (2009) is used. Bringi et al. (2009) suggested a line in the  $N_w$ - $D_0$  plane, where  $D_0$  is the median volume diameter, that separates the convective and stratiform rain types, which is expressed by

$$\log_{10}(N_w^{\text{sep}}) = -1.6D_0 + 6.3 \quad (18)$$

Using Eq. (13), they suggested the likelihood index  $I$ , which is defined as

$$I = \log_{10}(N_w) - \log_{10}(N_w^{\text{sep}}) \quad (19)$$

Thurai et al. (2016) classified the rain type of 1-min disdrometer data using  $I$ . When  $I < -0.3$  ( $I > 0.3$ ), the 1-min disdrometer data is identified as convective (stratiform) rain; otherwise, it is classified as mixed rain.

## 2.3 Reanalysis data

To investigate the thermodynamical and cloud characteristics at each site which may be associated with the RSD characteristics at the site, the reanalysis version 5 from the European Centre for Medium-Range Weather Forecasts (ERA5, Hersbach et al. 2020) with 1-h temporal resolution and  $0.25^\circ \times 0.25^\circ$  horizontal resolution is used. The convective available potential energy (CAPE), cloud-base height, cloud fraction, and hydrometeor mass contents in the ERA5 data at the grid point which is closest to each of the disdrometer sites are used. In addition, cloud-top height is obtained by identifying the topmost grid where the cloud fraction is greater than 0.01 and the total mass content of hydrometeors is greater than  $10^{-3} \text{ g kg}^{-1}$ .

**Fig. 2** Scatter plots of hourly accumulated rainfall amount observed by the disdrometers and rain gauges in **a** Seoul, **b** Chuncheon, and **c** Jincheon

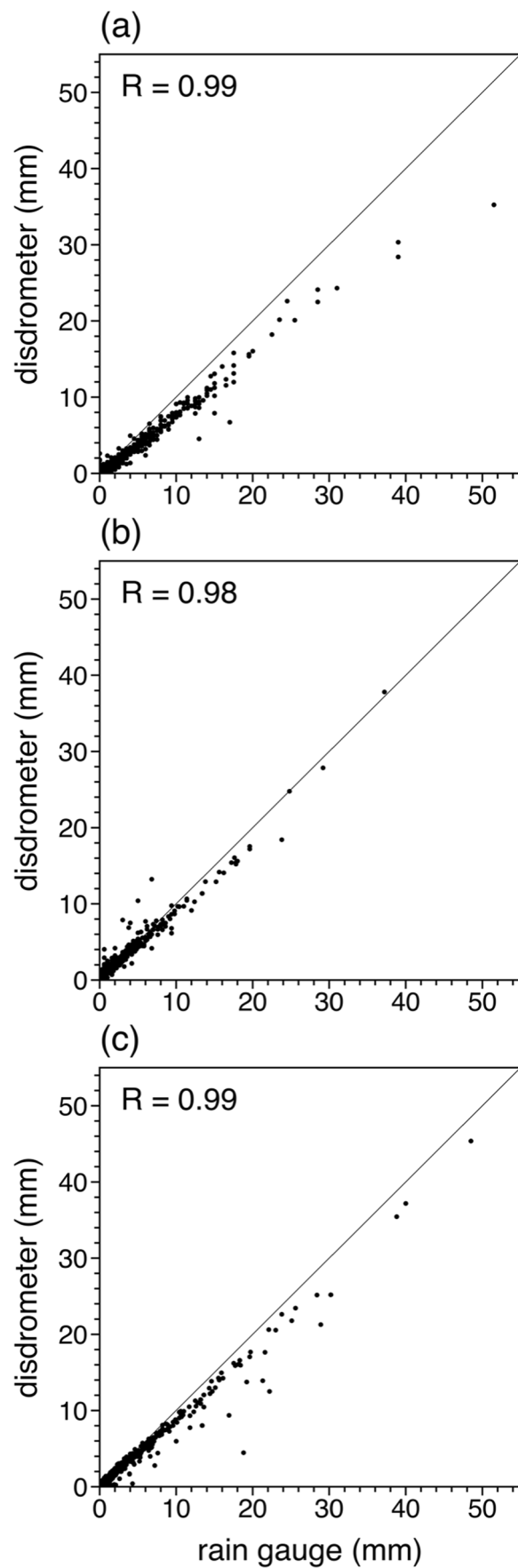
### 3 Results and discussion

#### 3.1 Regional differences in precipitation and RSD characteristics

To examine the differences in precipitation characteristics among the three sites, the accumulated rainfall amount and accumulated rainfall duration are shown in Fig. 3a. The accumulated rainfall amount (duration) is 2568 mm (889 h) for Seoul, 2697 mm (880 h) for Chuncheon, and 2845 mm (1090 h) for Jincheon. Jincheon exhibits the largest accumulated rainfall amount and duration, but the mean rainfall intensity calculated by dividing the accumulated rainfall amount by the accumulated rainfall duration is  $2.6 \text{ mm h}^{-1}$ , which is the smallest among the three sites. Seoul and Chuncheon have similar accumulated rainfall durations, but Chuncheon has a larger accumulated rainfall amount than Seoul. This indicates that the mean rainfall intensity in Chuncheon ( $3.1 \text{ mm h}^{-1}$ ) is greater than that in Seoul ( $2.9 \text{ mm h}^{-1}$ ).

Figure 3b shows the box plot of rain rate for rainfall events at each site. Here, a single rainfall event is composed of a set of consecutive 1-min disdrometer data, and the rain rate is obtained for each event. The numbers of rainfall events in Seoul, Chuncheon, and Jincheon are 1958, 1730, and 2109, respectively. The rain rate averaged over the rainfall events in Jincheon ( $1.6 \text{ mm h}^{-1}$ ) is smaller than those of Seoul ( $1.8 \text{ mm h}^{-1}$ ) and Chuncheon ( $1.9 \text{ mm h}^{-1}$ ). The 95th percentile of rain rate in Jincheon ( $6.0 \text{ mm h}^{-1}$ ) is also smaller than those in Seoul ( $8.2 \text{ mm h}^{-1}$ ) and Chuncheon ( $7.2 \text{ mm h}^{-1}$ ). The mean and 75th percentile of rain rate in Seoul are smaller than those in Chuncheon, but the 95th percentile of rain rate in Seoul is larger than that in Chuncheon. This suggests that the rainfall in Chuncheon is stronger on average than that in Seoul, but Seoul experiences more extreme rainfall events than Chuncheon.

Figure 4a shows the RSD for each site, obtained by averaging those from 1-min disdrometer data. The raindrop number concentration in Jincheon peaks at  $D=0.437 \text{ mm}$ , while those in Seoul and Chuncheon both peak at larger  $D$  ( $0.562 \text{ mm}$ ). For smaller diameters, the raindrop number concentrations in Seoul and Chuncheon sharply decrease, being about 1-order smaller than that in Jincheon for the smallest-diameter bin ( $D=0.25\text{--}0.375 \text{ mm}$ ). As the diameter increases from the RSD peaks, the raindrop number concentrations at all sites decrease almost exponentially, which resemble the Marshall-Palmer distribution (Marshall and Palmer 1948). Chuncheon shows the largest raindrop number concentration for  $D=1\text{--}3 \text{ mm}$ . Seoul shows the largest



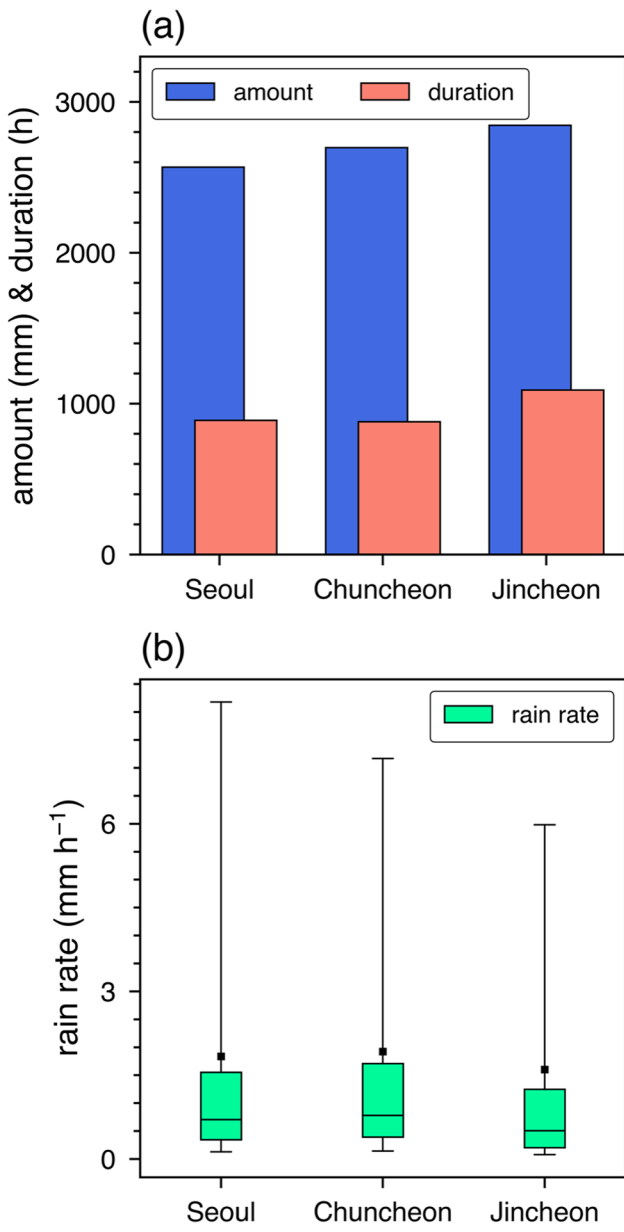


**Fig. 3** **a** Accumulated rainfall amount and duration and **b** box plot of rain rate for rainfall events at each site. The upper boundary, centerline, and lower boundary of the boxes represent the 75th, 50th, and 25th percentiles, respectively. The upper and lower whiskers indicate the 95th and 5th percentiles, respectively. The black squares in the box plots represent the mean value

raindrop number concentration for  $D \geq 3$  mm, and the difference from those at other two sites is prominent especially for  $D \geq 6$  mm. Figure 4b shows the normalized  $R(D)$  for each site, obtained by averaging those from 1-min disdrometer data and normalizing by the total rain rate. The area under the normalized  $R(D)$  curve indicates the contribution of the raindrops in each diameter bin to the total rain rate. Jincheon shows a greater contribution of small raindrops to the total rain rate than the other two sites: the area under the

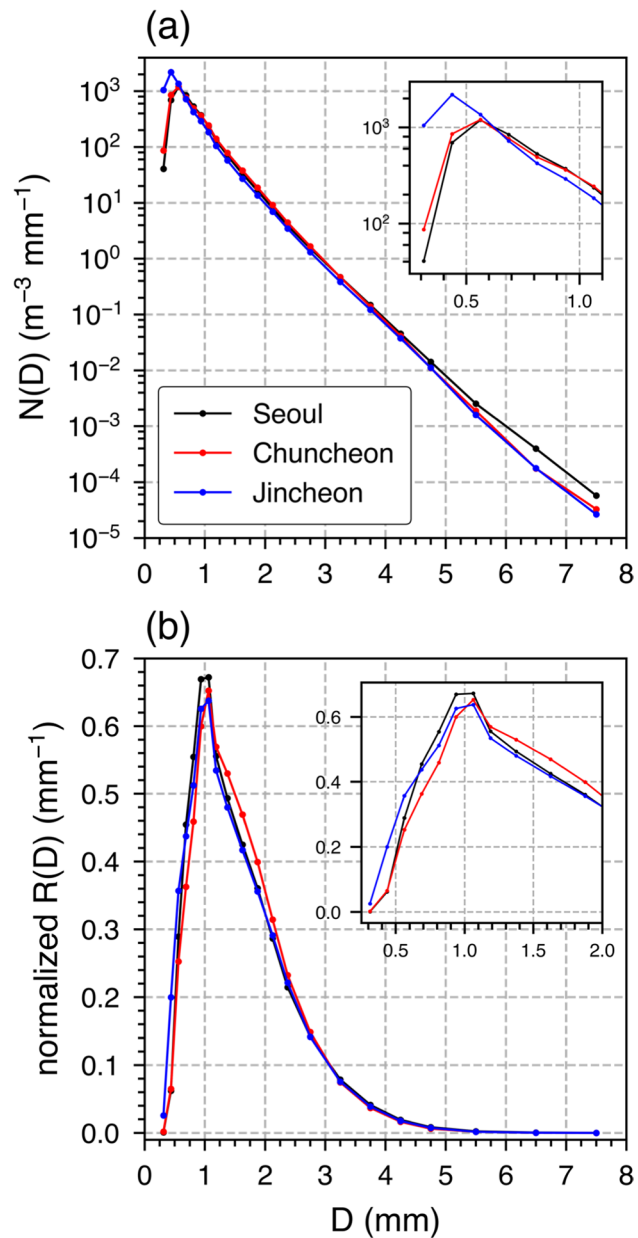
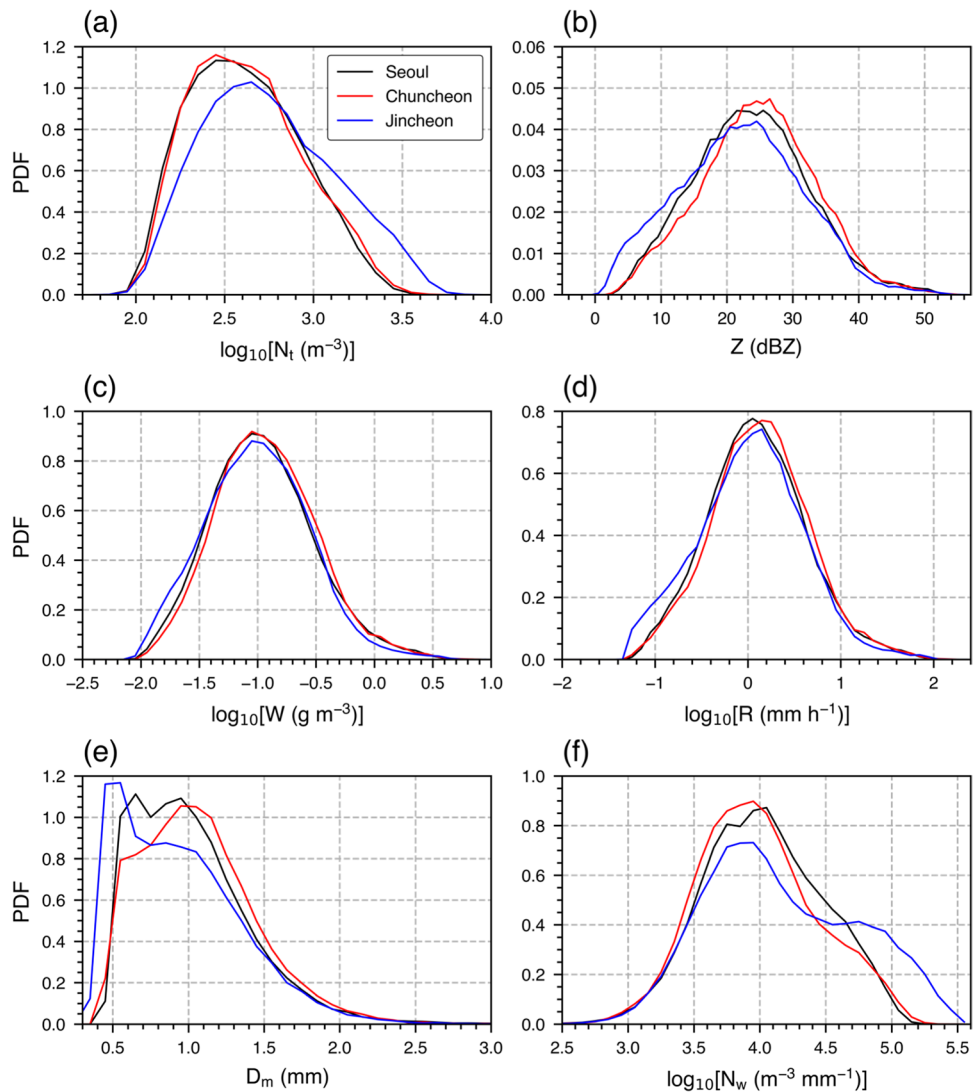


**Fig. 4** **a** Raindrop size distribution and **b** normalized  $R(D)$  at each site

normalized  $R(D)$  curve for  $D = 0.25\text{--}0.625$  mm is 0.07 in Jincheon, which is larger than those in Seoul and Chuncheon (0.04 and 0.04). Another notable difference is found at  $D = 1.125\text{--}3$  mm. For this diameter range that is responsible for a large portion of the total rain rate, Chuncheon shows the largest area under the normalized  $R(D)$  curve (0.63), followed by Seoul (0.59) and Jincheon (0.58).

The differences in RSD characteristics among the three sites can be better shown by looking into the probability density functions (PDFs) for RSD parameters. Figure 5 shows the PDFs of the logarithm of total raindrop number

**Fig. 5** Probability density functions of **a**  $\log_{10}N_t$ , **b**  $Z$ , **c**  $\log_{10}W$ , **d**  $\log_{10}R$ , **e**  $D_m$ , and **f**  $\log_{10}N_w$  for each site



concentration  $\log_{10}N_t$ , the radar reflectivity  $Z$ , the logarithm of rainwater content  $\log_{10}W$ , the logarithm of rain rate  $\log_{10}R$ , the mass-weighted diameter  $D_m$ , and the logarithm of generalized intercept parameter  $\log_{10}N_w$  at each site. The mean and standard deviation values of the six RSD parameters are given in Table 1. The PDFs of  $\log_{10}N_t$  are positively skewed at all sites. Jincheon's PDF of  $\log_{10}N_t$  is highly distinguishable from those of Seoul and Chuncheon,

showing a peak at larger  $\log_{10}N_t$  (2.65) than the other two sites (2.45 for both Seoul and Chuncheon). Also, the  $\log_{10}N_t$  PDF in Jincheon is more widely distributed than the others: the standard deviation of  $\log_{10}N_t$  in Jincheon (0.37) is larger than those in Seoul (0.31) and Chuncheon (0.31). This is associated with the much larger PDF in Jincheon for  $\log_{10}N_t > 3$ . For  $Z$ , Chuncheon shows the largest mean value (24.73 dBZ), followed by Seoul (23.74 dBZ) and Jincheon

**Table 1** Mean and standard deviation (in parentheses) values of RSD parameters for each site. The units of  $N_t$ ,  $Z$ ,  $W$ ,  $R$ ,  $D_m$ , and  $N_w$  are  $m^{-3}$ ,  $dBZ$ ,  $g m^{-3}$ ,  $mm h^{-1}$ ,  $mm$ , and  $m^{-3} mm^{-1}$ , respectively

Site data #	$\log_{10}N_t$	$Z$	$\log_{10}W$	$\log_{10}R$	$D_m$	$\log_{10}N_w$
Seoul 53,340	2.61 (0.31)	23.74 (8.69)	-0.96 (0.44)	0.10 (0.53)	1.02 (0.38)	4.03 (0.45)
Chuncheon 52,787	2.63 (0.31)	24.73 (8.58)	-0.92 (0.43)	0.14 (0.53)	1.07 (0.38)	3.99 (0.45)
Jincheon 65,405	2.75 (0.37)	22.02 (9.43)	-1.00 (0.44)	0.03 (0.57)	0.95 (0.41)	4.16 (0.57)

(22.02 dBZ). The PDF of  $Z$  in Chuncheon is least positively skewed, showing the largest values for  $22 \text{ dBZ} < Z < 42 \text{ dBZ}$  among the three sites. This suggests that Chuncheon experiences the most frequent appearance of large raindrops. In contrast, Jincheon shows the largest PDF for  $Z < 16 \text{ dBZ}$  among the three sites. The PDFs of  $\log_{10}W$  and  $\log_{10}R$  where Jincheon shows large values for small  $W$  and  $R$ , respectively, reflect the higher frequency of light rain in Jincheon than in Seoul and Chuncheon.

The PDFs of  $D_m$  and  $\log_{10}N_w$  show clear differences among the three sites. The PDF of  $D_m$  in Jincheon peaks at  $D_m = 0.55 \text{ mm}$ , drops at  $D_m = 0.55\text{--}0.65 \text{ mm}$ , and plateaus until  $D_m = 1.1 \text{ mm}$ . The high frequency of small  $D_m$  may be associated with the high frequency of light rain in Jincheon. The PDF of  $D_m$  in Seoul shows a bimodal distribution, peaking at  $D_m = 0.65$  and  $0.95 \text{ mm}$ . Chuncheon shows the PDF of  $D_m$  that peaks at much larger  $D_m$  ( $0.95 \text{ mm}$ ) than that in Jincheon, and also shows the largest PDF for  $D_m = 1.0\text{--}2.4 \text{ mm}$  among the three sites. The PDF of  $\log_{10}N_w$  in Jincheon shows a peak at  $\log_{10}N_w = 3.95$  and a plateau in the range of  $\log_{10}N_w = 4.4\text{--}4.9$ . The former is related to the plateau in the  $D_m$  PDF for  $D_m = 0.7\text{--}1.1 \text{ mm}$  and the latter is related to the peak at  $D_m = 0.55 \text{ mm}$ . The PDFs of  $\log_{10}N_w$  in Seoul and Chuncheon show their maxima at 4.05 and 3.95, respectively.

### 3.2 RSD characteristics according to the rain type and rain rate and their regional differences

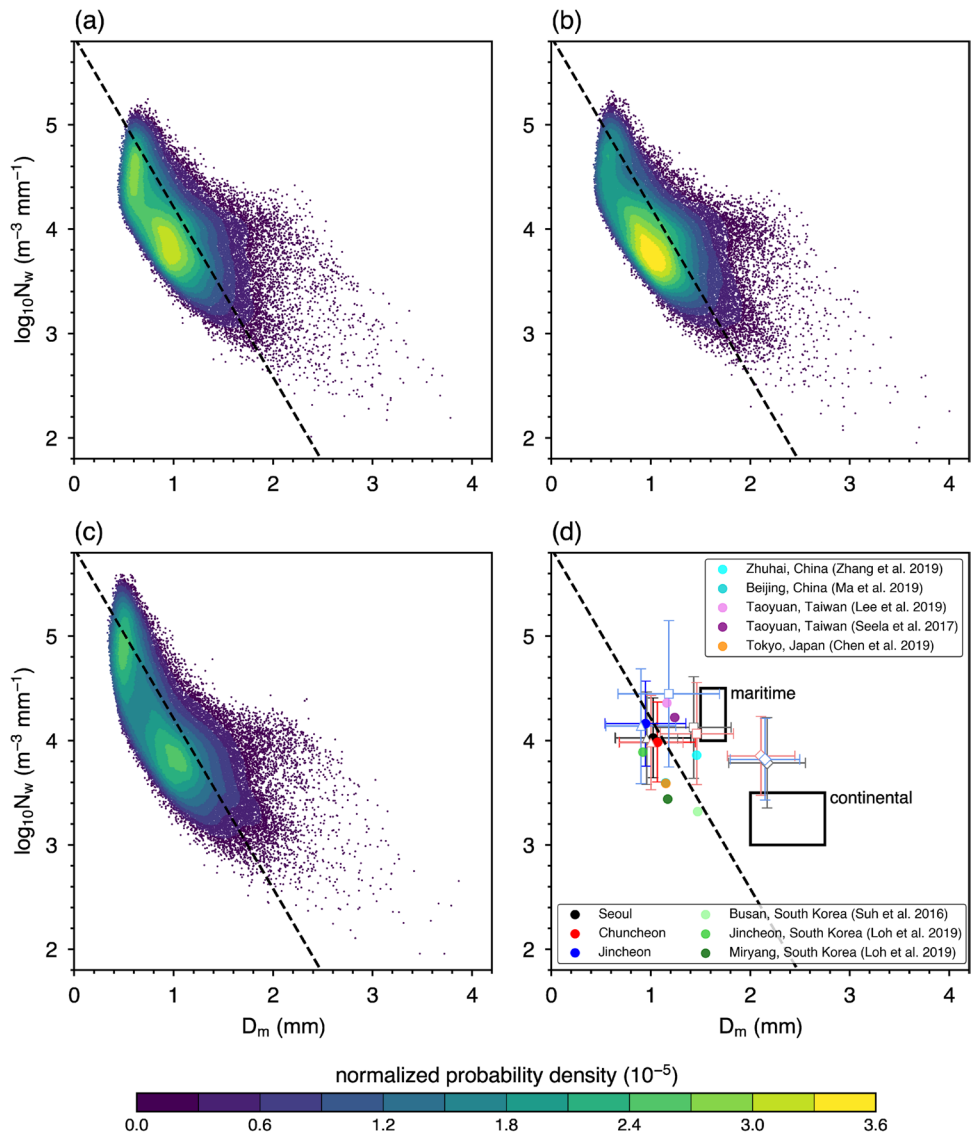
In this subsection, the RSD characteristics at each site are examined according to the rain rate and rain type and their differences among the three sites are investigated. Figure 6a–c shows the density scatter plots of  $D_m$  and  $\log_{10}N_w$  at each site, where the  $D_m\text{--}\log_{10}N_w$  line that was obtained through the least square fitting of stratiform rain data by Bringi et al. (2003) is indicated. At all sites, a large portion of data appear near or below the stratiform line, indicating that stratiform rain dominates the precipitation. All three sites show a peak of probability density at  $D_m = 0.8\text{--}1.2 \text{ mm}$  and  $\log_{10}N_w = 3.6\text{--}4.2$ . In addition to this peak, Jincheon shows a prominent peak at  $D_m = 0.4\text{--}0.6 \text{ mm}$  and  $\log_{10}N_w = 4.6\text{--}5.1$ , and the probability densities of the two peaks are similar. The two peaks explain the distinctive distributions of  $D_m$  and  $\log_{10}N_w$  PDFs in Jincheon, each of which has a peak and a plateau (Fig. 5e and f). This peak does not appear in Chuncheon. Seoul shows a secondary peak at  $D_m = 0.5\text{--}0.7 \text{ mm}$  and  $\log_{10}N_w = 4.2\text{--}4.8$ , but its probability density is much smaller than that of the primary peak.

Figure 6d shows the mean and standard deviation values of  $D_m$  and  $\log_{10}N_w$  at each site for the total and each rain type, where two boxes represent the clusters of maritime-like convective rain and continental-like convective

rain proposed by Bringi et al. (2003). For the total data, the mean  $D_m\text{--}\log_{10}N_w$  pair at each site appears near the stratiform line and within the range of the primary peak ( $D_m = 0.8\text{--}1.2 \text{ mm}$  and  $\log_{10}N_w = 3.6\text{--}4.2$ ) in the  $D_m\text{--}\log_{10}N_w$  density scatter plots (Fig. 6a–c). Jincheon shows the smallest mean  $D_m$  (0.95 mm) and largest mean  $\log_{10}N_w$  (4.16), while Chuncheon shows the largest mean  $D_m$  (1.07 mm) and smallest mean  $\log_{10}N_w$  (3.99). The mean  $D_m\text{--}\log_{10}N_w$  pair for stratiform rain also appear near the stratiform line, which is similar to those for the total, because stratiform rain accounts for about 90% of the total. For mixed rain, the mean  $D_m\text{--}\log_{10}N_w$  pair in Jincheon largely deviates from those in Seoul and Chuncheon. The mean  $D_m\text{--}\log_{10}N_w$  pair in Jincheon is in an intermediate position between the stratiform line and the cluster of maritime-like convective rain, while those in Seoul and Chuncheon are close to the cluster of maritime-like convective rain. For convective rain, the mean  $D_m\text{--}\log_{10}N_w$  pairs at all three sites are in intermediate positions between the clusters of maritime-like convective rain and continental-like convective rain. The difference among the three sites for convective rain is relatively small compared to that for the other rain types.

In Fig. 6d, mean  $D_m$  and  $\log_{10}N_w$  obtained at many other locations in East Asia are also presented. Compared to the mean  $D_m\text{--}\log_{10}N_w$  pair in Jincheon obtained in this study, that obtained by Loh et al. (2019) for the same site shows similar mean  $D_m$  (0.92 mm) but somewhat smaller  $\log_{10}N_w$  (3.89), which may be because Loh et al. (2019) obtained them from only twelve selected rainfall cases. Miryang (Loh et al. 2019), located in the southeastern region of South Korea, shows  $\log_{10}N_w$  (3.44) that is much smaller than the three sites examined in this study and  $D_m$  (1.17 mm) that is comparable to that in Seoul (1.02 mm) and Chuncheon (1.06 mm). Busan (Suh et al. 2016), a coastal city of South Korea located farther southeast from the three sites examined in this study, shows  $\log_{10}N_w$  further smaller than that in Miryang and  $D_m$  much larger than those in the other South Korean cities. Busan exhibits the longest distance in the  $D_m\text{--}\log_{10}N_w$  space from the three sites examined in this study, even longer than that for any other city in East Asia presented in Fig. 6d, which indicates that South Korea has a very large variability of RSD characteristics within the country. Beijing (Ma et al. 2019) and Tokyo (Chen et al. 2019) show almost identical mean  $D_m$  and  $\log_{10}N_w$ , and the mean  $D_m\text{--}\log_{10}N_w$  pair is below the stratiform line, as in the South Korean cities. Mean  $D_m$  in the two cities (1.15 and 1.15 mm) are comparable to that in Seoul and Chuncheon and mean  $\log_{10}N_w$  in the two cities (3.60, 3.59) are smaller than that in the three sites examined in this study. Taoyuan (Seela et al. 2017; Lee et al. 2019) and Zhuhai (Zhang et al. 2019), coastal cities located at much lower latitudes than the aforementioned cities, show the mean RSD characteristics that are

**Fig. 6** Density scatter plots of the mass-weighted diameter and the logarithm of generalized intercept parameter for **a** Seoul, **b** Chuncheon, and **c** Jincheon. **d** Shows the mean values of  $D_m$  and  $\log_{10}N_w$  for the total (filled circles), stratiform rain (triangles), mixed rain (squares), and convective rain (diamonds) at each site with their standard deviation (whiskers). The mean values obtained in previous studies for East Asia are represented by different color dots in **d**. Note that the dots of Ma et al. (2019) and Chen et al. (2017) overlap each other. The black dashed line represents the stratiform line proposed by Bringi et al. (2003). The two boxes in **d** represent the maritime-like convective rain and continental-like convective rain proposed by Bringi et al. (2003), respectively



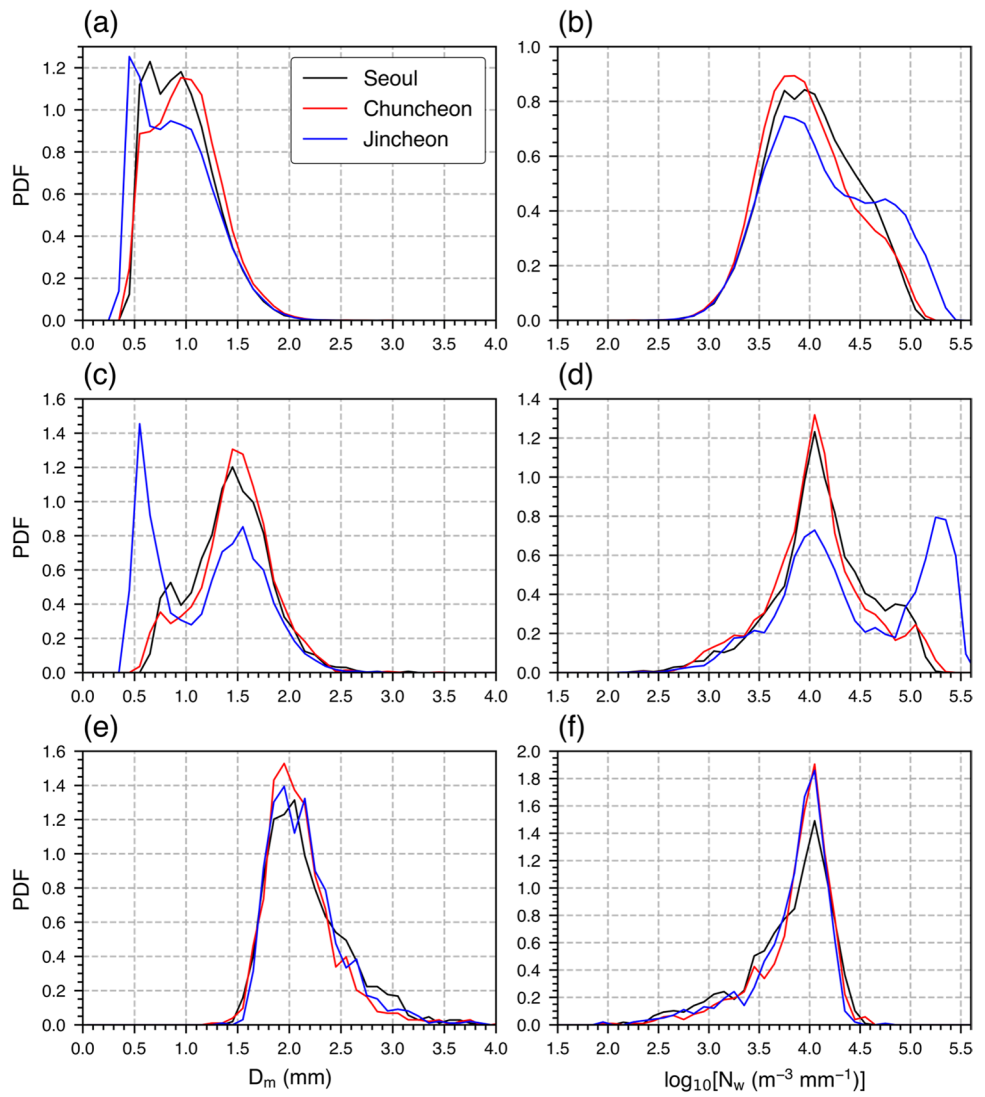
closer to those of maritime-like convective precipitation than any other city.

Among the three sites, Seoul shows the largest proportion of convective rain, Chuncheon shows the largest proportion of mixed rain, and Jincheon shows the largest proportion of stratiform rain. In terms of the precipitation amount, the stratiform, mixed, and convective rain respectively account for 47.4%, 27.9%, 24.7% in Seoul; 47.3%, 28.6%, and 24.1% in Chuncheon; and 49.6%, 27.0%, and 23.4% in Jincheon.

Figure 7 shows the PDFs of  $D_m$  and  $\log_{10}N_w$  for each rain type at each site. For stratiform rain, as in the PDF without the rain-type classification (Fig. 5e), the  $D_m$  value at which the PDF is maximized is smallest (0.45) in Jincheon and largest (0.95) in Chuncheon. Jincheon shows a distinct shape of  $\log_{10}N_w$  PDF, which is relatively high at large  $\log_{10}N_w$  compared to the other sites. In contrast, Chuncheon shows relatively high PDF at small  $\log_{10}N_w$

compared to the other sites. For both  $D_m$  and  $\log_{10}N_w$ , Seoul shows somewhat intermediate distributions of PDF between Chuncheon and Jincheon. For convective rain, all sites have similar distributions of PDFs of  $D_m$  and  $\log_{10}N_w$ . Compared to stratiform rain, the PDF of  $D_m$  for convective rain is distributed mainly at much larger  $D_m$  and the PDF of  $\log_{10}N_w$  at large  $\log_{10}N_w$  is very low. The distributions of PDFs of  $D_m$  and  $\log_{10}N_w$  for convective rain in Seoul are more dispersed than those in Chuncheon and Jincheon, showing overall higher PDF at large  $D_m$  ( $2.45 \text{ mm} < D_m < 3.05 \text{ mm}$ ) and at small  $\log_{10}N_w$  ( $2.45 < \log_{10}N_w < 3.65$ ). For mixed rain, the PDFs of  $D_m$  at all sites have double-peak structures where the peak on the left side is close to the peak of  $D_m$  PDF for stratiform rain and the peak on the right side is close to the peak of  $D_m$  PDF for convective rain. This double-peak structure of  $D_m$  PDF for mixed rain is also reported by Jwa et al. (2021)

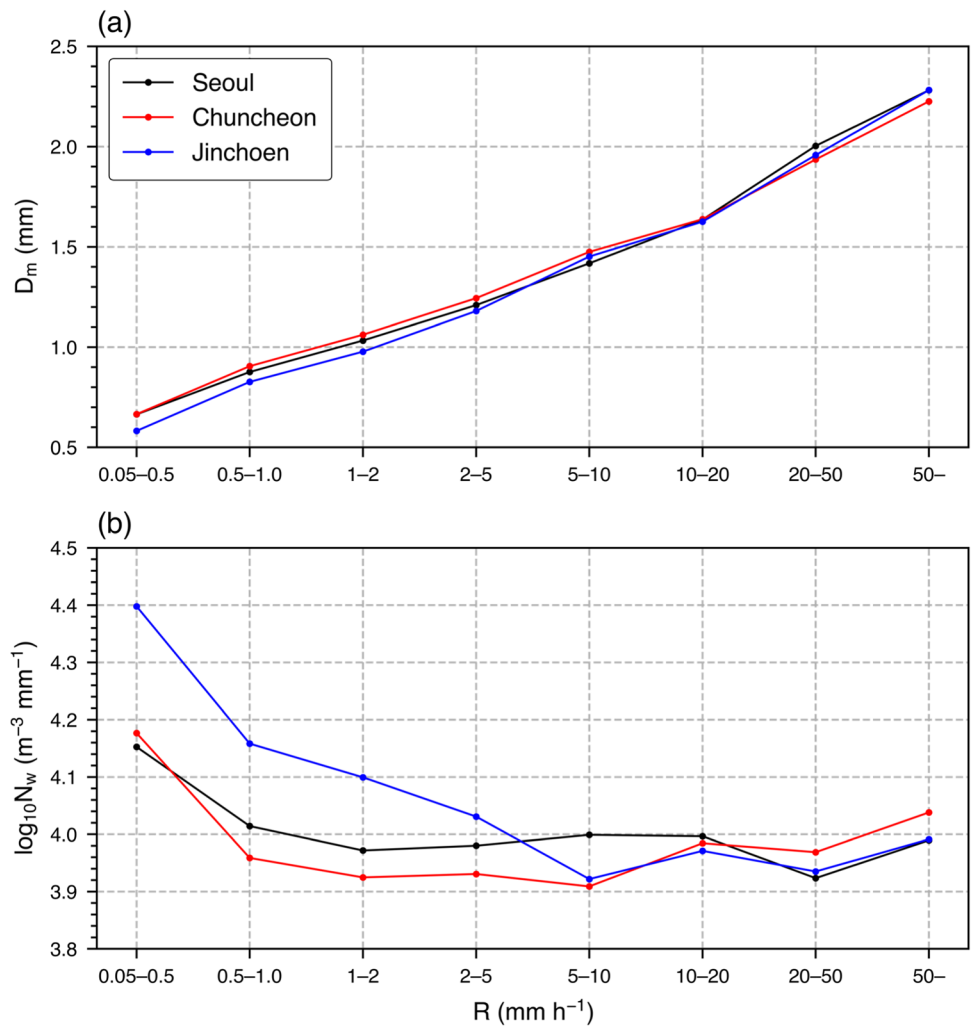
**Fig. 7** Probability density functions of **a, c, e** the mass-weighted mean diameter and **b, d, f** the logarithm of generalized intercept parameter for **a, b** stratiform, **c, d** mixed, and **e, f** convective rain at each site



who examined the RSD characteristics in Seoul, and they suggested that the two peaks are associated with different weather types which are the Changma front and the low-pressure system. They showed that the RSD characteristic of mixed rain of the Changma front resembles that of convective rain, while the RSD characteristic of mixed rain of the low-pressure system resembles that of stratiform rain. In Jincheon, the stratiform-like peak is higher than the convective-like peak, while it is the opposite in Seoul and Chuncheon. For  $\log_{10}N_w$ , Jincheon again shows a different shape of PDF where the PDF is maximized at  $\log_{10}N_w = 5.25$ , while it is maximized at  $\log_{10}N_w = 4.05$ , which is the same as the  $\log_{10}N_w$  value for the PDF peak for convective rain, in Seoul and Chuncheon. The distinct two peaks of  $\log_{10}N_w$  PDF for mixed rain in Jincheon are closely linked to the distinct two peaks of  $D_m$  PDF. The left (right) peak among the former corresponds to the right (left) peak among the latter.

To further investigate the differences in RSD characteristics among the three sites, the relationship between the rain rate and  $D_m$  and that between the rain rate and  $\log_{10}N_w$  at each site are presented in Fig. 8.  $D_m$  and  $\log_{10}N_w$  are averaged for each of the eight rain rate categories, which is  $0.05 \text{ mm h}^{-1} \leq R < 0.5 \text{ mm h}^{-1}$ ,  $0.5 \text{ mm h}^{-1} \leq R < 1.0 \text{ mm h}^{-1}$ ,  $1 \text{ mm h}^{-1} \leq R < 2 \text{ mm h}^{-1}$ ,  $2 \text{ mm h}^{-1} \leq R < 5 \text{ mm h}^{-1}$ ,  $5 \text{ mm h}^{-1} \leq R < 10 \text{ mm h}^{-1}$ ,  $10 \text{ mm h}^{-1} \leq R < 20 \text{ mm h}^{-1}$ ,  $20 \text{ mm h}^{-1} \leq R < 50 \text{ mm h}^{-1}$ , and  $50 \text{ mm h}^{-1} \leq R$ . At all sites,  $D_m$  increases as the rain rate increases. For the rain rate in the range of  $0.05 - 5 \text{ mm h}^{-1}$ , Jincheon shows the smallest  $D_m$ . Chuncheon shows the largest  $D_m$  for the rain rate in the range of  $0.05 - 20 \text{ mm h}^{-1}$  and the smallest  $D_m$  for the rain rate larger than  $20 \text{ mm h}^{-1}$ . The relationship between the rain rate and  $\log_{10}N_w$  is not monotonic at all sites. For the rain rate in the range of  $0.05 - 5 \text{ mm h}^{-1}$ , Jincheon shows the largest  $\log_{10}N_w$  among the three sites. For the rain rate larger than  $20 \text{ mm h}^{-1}$ ,

**Fig. 8** **a** Mass-weighted mean diameter and **b** logarithm of generalized intercept parameter averaged over RSD data in each rain rate category at each site



Chuncheon shows the largest  $\log_{10} N_w$ . The above relationships between the rain rate and the two RSD parameters indicate that light precipitation in Jincheon consists of a relatively large number of relatively small raindrops compared to light precipitation in the other sites and that very heavy precipitation in Chuncheon consists of a relatively small raindrops compared to very heavy precipitation in the other sites. Very heavy precipitation in Seoul consists of relatively large raindrops compared to very heavy precipitation in Chuncheon.

The above analyses in subsections 3.1 and 3.2 reveal the differences in precipitation and RSD characteristics among the three cities in South Korea. Jincheon, the least populated and southernmost city among the three cities, is characterized by the smallest mean rainfall intensity with a relatively high frequency of light rain, which is associated with the smallest  $D_m$  and largest  $\log_{10} N_w$ . In contrast, Chuncheon, a medium-sized city located in a basin, is characterized by the largest mean rainfall intensity with a relatively high frequency of heavy rain, which is associated with the largest

$D_m$  and smallest  $\log_{10} N_w$ . Seoul, the most populated city in South Korea, is characterized by the intermediate mean rainfall intensity associated with the intermediate  $D_m$  and  $\log_{10} N_w$  between those in Chuncheon and Jincheon. Distinctive features of the precipitation and RSD characteristics in Seoul are that although the mean rainfall intensity is weaker and the mean  $D_m$  is smaller than those in Chuncheon, extreme rainfall events occur more frequently and  $D_m$  for very heavy rain is larger compared to Chuncheon. In the next subsection, possible causes for these regional differences in RSD characteristics are investigated.

### 3.3 Regional differences in thermodynamic and cloud characteristics

The regional differences in thermodynamical and cloud microphysical characteristics that may be responsible for regional differences in RSD characteristics are examined. Figure 9 shows the box plots of the convective available potential energy (CAPE), cloud-top height, and cloud-base

**Fig. 9** Box plots of **a** convective available potential energy, **b** cloud-top height, and **c** cloud-base height at each site. The upper boundary, centerline, and lower boundary of the boxes represent the 75th, 50th, and 25th percentiles, respectively. The upper and lower whiskers indicate the 95th and 5th percentiles, respectively. The black squares in the box plots represent the mean value

height at each site. The median and 75th and 95th percentiles of CAPE in Jincheon are smallest among those in the three sites, indicating that Jincheon has the least thermodynamical potential of development of strong convection, which is also supported by the overall lowest cloud-top height. Because relatively weak convective activities in clouds may lead to relatively insufficient growth of hydrometeor particles due to less interaction with each other, the overall smallest CAPE and lowest cloud-top height in Jincheon can be responsible for the smallest  $D_m$ . Compared to Jincheon, Chuncheon shows noticeably larger mean and 75th and 95th percentiles of CAPE and higher cloud-top height, which implies stronger convective activities in clouds that may be associated with the substantially larger  $D_m$ . The  $D_m$  difference between Jincheon and Chuncheon is similar to that between Palau and Taiwan reported by Seela et al. (2017), who also attributed the difference to the stronger convective activity in Taiwan than in Palau. In addition, the cloud-base height is lowest in Chuncheon. The low cloud-base height indicates less evaporation of raindrops below the cloud base and thus results in the larger sizes of raindrops at the surface. Seoul shows the largest 75th and 95th percentiles of CAPE. This can be associated with the most frequent occurrence of extreme rainfall events in Seoul. Compared to Chuncheon, the cloud-top height is overall similar but the cloud-base height is overall much higher, which may be responsible for the smaller mean  $D_m$ .

### 3.4 Implications for quantitative precipitation estimations and cloud microphysics parameterizations

From RSD data, some relations between RSD parameters that are useful for quantitative precipitation estimations and cloud microphysics parameterizations can be obtained. One example is the radar reflectivity–rain rate ( $Z$ – $R$ ) relation that can be used to estimate surface rain rate from radar observation. The power-law fitted  $Z$ – $R$  relations ( $Z = aR^b$ ) at the three sites are compared in Fig. 10. The exponent  $b$  in the  $Z$ – $R$  relation is similar among the three sites (1.56–1.59), while the coefficient  $a$  varies from 144 in Jincheon to 182 in Chuncheon (Fig. 10a). Up to  $Z = 68$  dBZ, rain rate is smallest in Chuncheon and largest in Jincheon for the same radar reflectivity. For example, for  $Z = 45$  dBZ, rain rate is as small as  $27.3 \text{ mm h}^{-1}$  in Chuncheon and as large as  $29.7 \text{ mm h}^{-1}$  in Jincheon,

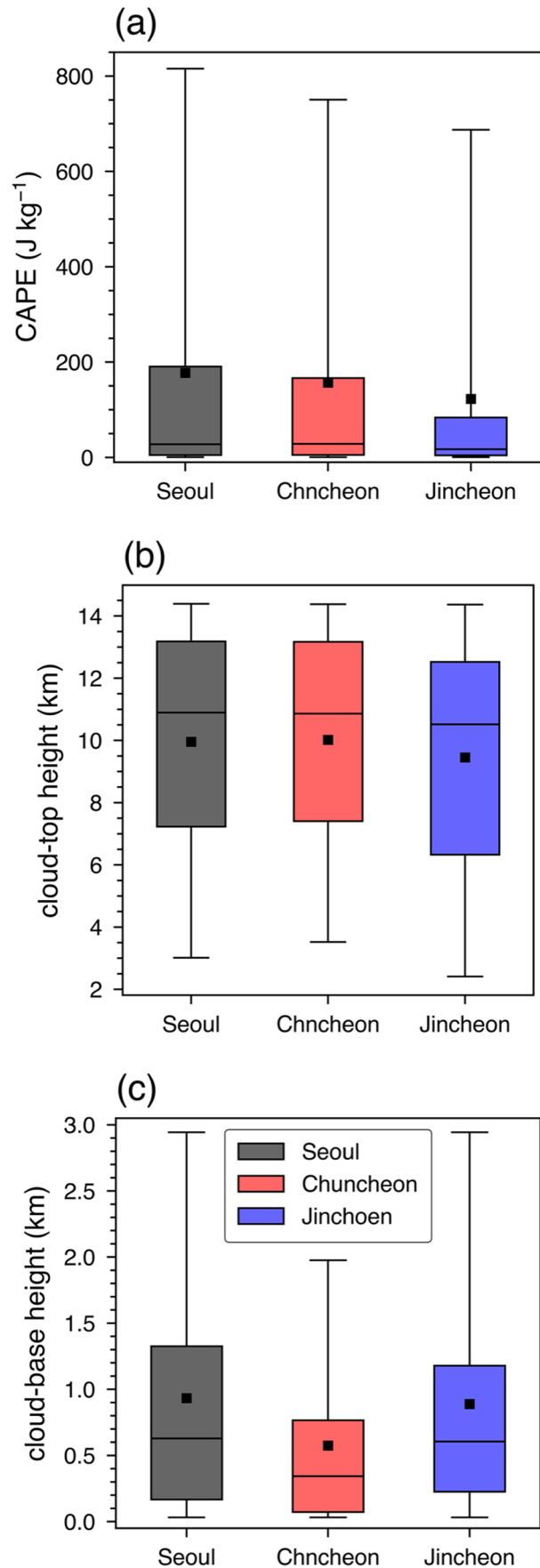
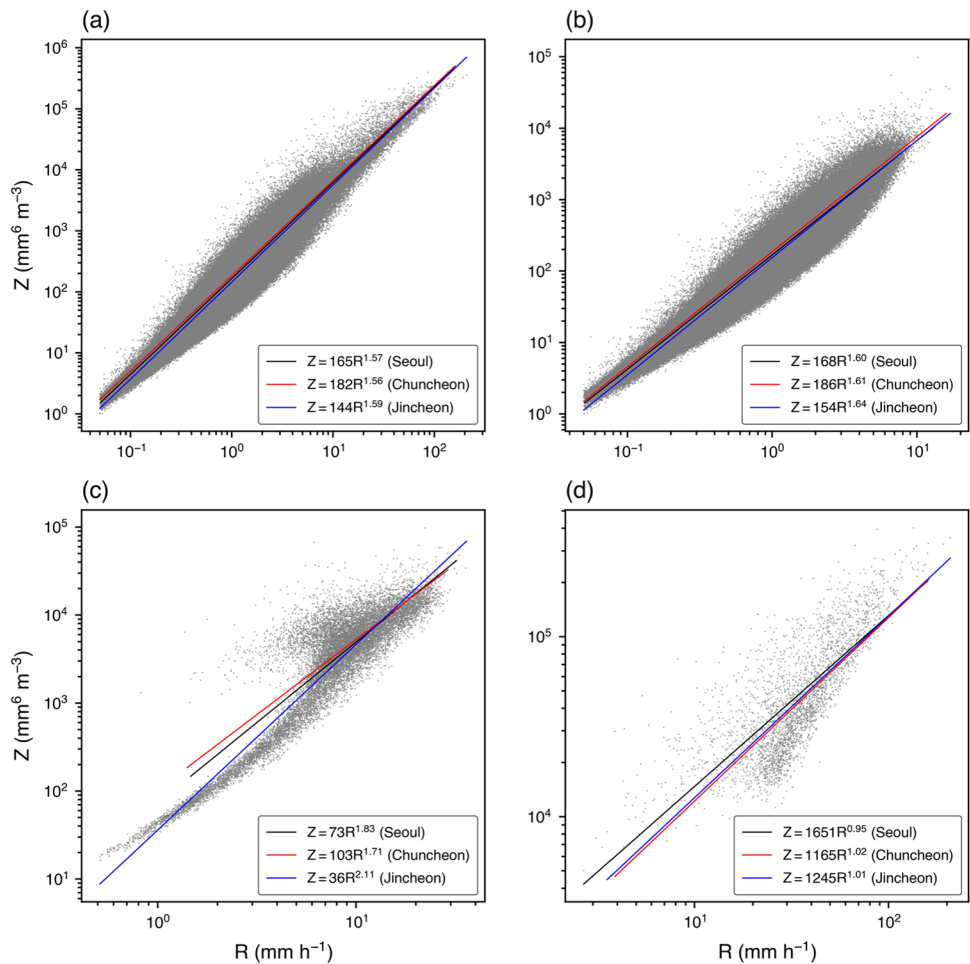


**Fig. 10** Scatter plot of the rain rate  $R$  and the radar reflectivity  $Z$  for **a** the total, **b** stratiform rain, **c** mixed rain, and **d** convective rain. The black, red, and blue lines represent the power-law fitted  $Z$ - $R$  relations for Seoul, Chuncheon, and Jincheon, respectively



differing by  $2.4 \text{ mm h}^{-1}$ . The exponent  $b$  at the three sites is mostly larger than that in the southern region of South Korea (1.41–1.61 for stratiform rain and 1.39–1.48 for convective rain) obtained by Suh et al. (2021), and it is rather close to that in summertime Beijing (1.57) obtained by Ma et al. (2019). That Chuncheon shows the largest  $a$  among the three sites is consistent with the finding of Suh et al. (2021) that  $a$  is larger at inland sites than at coastal sites in the southern region of South Korea.

The features of the  $Z$ - $R$  relations at the three sites found for the total data are also found when the stratiform rain data only are considered. For stratiform rain, the three sites show  $b$  that is similar among them (1.60–1.64) and  $a$  that is smallest in Jincheon (154) and largest in Chuncheon (186) (Fig. 10b). The exponent  $b$  for stratiform rain is similar to that obtained by Marshall and Palmer (1948) for warm stratiform rain (1.6). Compared to stratiform rain, convective rain shows much smaller  $b$  (0.95–1.02) and much larger  $a$  (1165–1651) at all three sites (Fig. 10d). Smaller  $b$  and larger  $a$  for convective rain compared to stratiform rain are consistent with Marshall et al. (1955) who suggested  $Z=200R^{1.6}$  for stratiform rain and  $Z=300R^{1.4}$  for

convective rain, but the differences in this study are much more drastic. For convective rain, the coefficient  $a$  is smallest in Chuncheon, which is in contrast with its behavior for stratiform rain. Mixed rain shows most distinct differences among the three sites (Fig. 10c). For mixed rain, Chuncheon shows the largest  $a$  and smallest  $b$ , while Jincheon shows the smallest  $a$  and largest  $b$ .

The shape parameter–slope parameter ( $\mu$ - $\Lambda$ ) relation can be used to retrieve RSD when only limited information on RSD is given, which is the case for estimating rain rate from radar observation (Zhang et al. 2001) and for retrieving three-parameter gamma RSD from two prognostic RSD moments in double-moment cloud microphysics schemes (Morrison and Milbrandt 2015). The  $\mu$ - $\Lambda$  relation is known to vary with the location (see Table 8 in Seela et al. (2018) and Table 3 in Han et al. (2021)). Figure 11 shows the second-order polynomial fits for the  $\mu$ - $\Lambda$  relation at the three sites. Here, following Zhang et al. (2003), only the data with rain rate larger than  $5 \text{ mm h}^{-1}$  and with the total raindrop count larger than 1000 are considered. The  $\mu$ - $\Lambda$  relations at the three sites are overall similar to each other, which indicates a small spatial variability of the  $\mu$ - $\Lambda$

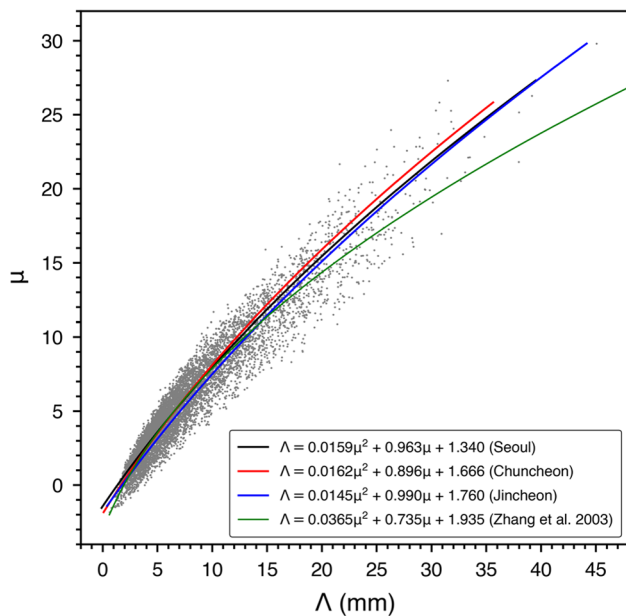


**Fig. 11** Scatter plot of the slope parameter  $\Lambda$  and the shape parameter  $\mu$ . The black, red, and blue lines represent the second-order polynomial fits for the  $\mu$ - $\Lambda$  relation for Seoul, Chuncheon, and Jincheon, respectively. The green line represents the  $\mu$ - $\Lambda$  relation obtained in Zhang et al. (2003)

relation within the northern–central region of South Korea. Han et al. (2021) also reported that the  $\mu$ - $\Lambda$  relation does not vary much within a small region. Nevertheless, the  $\mu$ - $\Lambda$  relations at the three sites deviate much from that in Florida obtained by Zhang et al. (2003), especially for large  $\Lambda$  for which  $\mu$  at the three sites are noticeably larger than that in Florida. Among the three sites, Jincheon exhibits the smallest  $\mu$  for a wide range of  $\Lambda$ . Wu et al. (2019) stated that a relatively small  $\mu$  for a given  $\Lambda$  may result from a relatively high number concentration of small raindrops, which seems to be the case in Jincheon.

## 4 Summary and conclusions

This study examined the differences in RSD characteristics among three cities (Seoul, Chuncheon, and Jincheon) in South Korea using disdrometer data for the period from 25 July 2018 to 31 July 2021 and the possible causes for the regional differences utilizing the ERA5 reanalysis data. Seoul is the most populated city in South Korea, Chuncheon is a medium-sized city located in a basin, and Jincheon is the least populated and southernmost city among the three cities. The three cities show clear differences in precipitation and RSD characteristics. Jincheon is characterized by the smallest mean rainfall intensity and a relatively high frequency of light rain, which are associated with the smallest  $D_m$  and the largest  $\log_{10}N_w$ . Chuncheon, on the other hand,

is characterized by the largest mean rainfall intensity and a relatively high frequency of heavy rain, which are associated with the largest  $D_m$  and the smallest  $\log_{10}N_w$ . The contrasts in RSD characteristics between the two cities can be attributable to the relatively large convective available potential energy, high cloud-top height, and low cloud-base height in Chuncheon compared to those in Jincheon. Seoul is characterized by the intermediate mean rainfall intensity associated with  $D_m$  and  $\log_{10}N_w$  that are intermediate between those in Jincheon and Chuncheon. In Seoul, extreme rainfall events occurs most frequently and  $D_m$  for very heavy rain is relatively large. This can be attributable to the most frequent occurrence of large convective available potential energy.

This study showed that the regional differences in RSD characteristics among the cities can be attributable to the regional differences in thermodynamic and cloud characteristics. Different urban characteristics and geographical characteristics of the cities can cause the differences in thermodynamic and cloud characteristics. Besides, as urban aerosols can serve as cloud condensation nuclei, different aerosol concentrations in the cities can cause differences in cloud microphysics among the cities. How these individual factors contribute to the regional differences in thermodynamical and cloud microphysical characteristics among the cities cannot be revealed under the analysis framework of this study, which is a limitation of this work. This deserves further investigation, in which various types of data such as radar observation data, satellite retrievals of cloud properties, atmospheric sounding data, and aerosol concentration data for each city need to be utilized.

**Acknowledgements** The authors are grateful to two anonymous reviewers for providing valuable comments on this work.

**Author contribution** Jong-Jin Baik designed this study. Joohyun Lee performed the data analysis and visualization. All authors discussed the results. Joohyun Lee and Han-Gyul Jin wrote the original draft. Jong-Jin Baik reviewed and edited the manuscript. All authors read and approved the final version of the manuscript.

**Funding** This work was supported by the Korea Meteorological Administration Research and Development Program under Grant KMI 2020-00710 and also by the National Research Foundation of Korea (2021R1A2C1007044).

**Data availability** The ERA5 data were downloaded from the Copernicus Climate Change Service (C3S) Climate Data Store (CDS).

**Code availability** The codes used for analyses in this study can be obtained from the corresponding author if necessary.

## Declarations

**Ethics approval** Not applicable.

**Consent to participate** Not applicable.

**Consent for publication** Not applicable.

**Conflict of interest** The authors declare no competing interests.

## References

- Angulo-Martínez M, Beguería S, Latorre B, Fernández-Raga M (2018) Comparison of precipitation measurements by OTT Parsivel<sup>2</sup> and Thies LPM optical disdrometers. *Hydrol Earth Syst Sci* 22:2811–2837
- Atlas D, Srivastava RC, Sekhon RS (1973) Doppler radar characteristics of precipitation at vertical incidence. *Rev Geophys* 11:1–35
- Bang W, Kwon S, Lee G (2017) Characteristic of raindrop size distribution using two-dimensional video disdrometer data in Daegu, Korea. *J Korean Earth Sci Soc* 38:511–521
- Bringi VN, Chandrasekar V, Hubbert J, Gorgucci E, Randeu WL, Schoenhuber M (2003) Raindrop size distribution in different climatic regimes from disdrometer and dual-polarized radar analysis. *J Atmos Sci* 60:354–365
- Bringi VN, Williams CR, Thurai M, May PT (2009) Using dual-polarized radar and dual-frequency profiler for DSD characterization: a case study from Darwin, Australia. *J Atmos Ocean Technol* 26:2107–2122
- Cao Q, Zhang G (2009) Errors in estimating raindrop size distribution parameters employing disdrometer and simulated raindrop spectra. *J Appl Meteorol Climatol* 48:406–425
- Chen B, Hu Z, Liu L, Zhang G (2017) Raindrop size distribution measurements at 4,500 m on the Tibetan Plateau during TIPEX-III. *J Geophys Res: Atmos* 122:11092–11106
- Chen Y, Duan J, An J, Liu H (2019) Raindrop size distribution characteristics for tropical cyclones and Meiyu-Baiu fronts impacting Tokyo, Japan. *Atmosphere* 10:391
- Dolan B, Fuchs B, Rutledge SA, Barnes EA, Thompson EJ (2018) Primary modes of global drop size distributions. *J Atmos Sci* 75:1453–1476
- Giangrande SE, Bartholomew MJ, Pope M, Collis S, Jensen MP (2014) A summary of precipitation characteristics from the 2006–11 northern Australian wet seasons as revealed by ARM disdrometer research facilities (Darwin, Australia). *J Appl Meteorol Climatol* 53:1213–1231
- Han Y, Guo J, Yun Y, Li J, Guo X, Lv Y, Wang D, Li L, Zhang Y (2021) Regional variability of summertime raindrop size distribution from a network of disdrometers in Beijing. *Atmos Res* 257:105591
- Hersbach H, Bell B, Berrisford P, Hirahara S, Horányi A, Muñoz-Sabater J, Nicolas J, Peubey C, Radu R, Schepers D, Simmons A, Soci C, Abdalla S, Abellán X, Balsamo G, Bechtold P, Bialetti G, Bidlot J, Bonavita M, De Chiara G, Dahlgren P, Dee D, Diamantakis M, Dragani R, Flemming J, Forbes R, Fuentes M, Geer A, Haimberger L, Healy S, Hogan RJ, Hölm E, Janisková M, Keeley S, Laloyaux P, Lopez P, Lupu C, Radnoti G, De Rosnay P, Rozum I, Vamborg F, Villaume S, Thépaut J-N (2020) The ERA5 global reanalysis. *Q J R Meteorol Soc* 146:1999–2049
- Jaffrain J, Berne A (2011) Experimental quantification of the sampling uncertainty associated with measurements from PAR-SIVEL disdrometers. *J Hydrometeorol* 12:352–370
- Jwa M, Jin H-G, Lee J, Moon S, Baik J-J (2021) Characteristics of raindrop size distribution in Seoul, South Korea according to rain and weather types. *Asia-Pacific J Atmos Sci* 57:605–617
- Kathiravelu G, Lucke T, Nichols P (2016) Rain drop measurement techniques: a review. *Water* 8:29
- Kim H-J, Lee K-O, You C-H, Uyeda H, Lee D-I (2019) Microphysical characteristics of a convective precipitation system observed on July 04, 2012, over Mt. Halla in South Korea. *Atmos Res* 222:74–87
- Lee M-T, Lin P-L, Chang W-Y, Seela BK, Janapati J (2019) Microphysical characteristics and types of precipitation for different seasons over North Taiwan. *J Meteorol Soc Jpn* 97:841–865
- Leinonen J, Moisseev D, Leskinen M, Petersen WA (2012) A climatology of disdrometer measurements of rainfall in Finland over five years with implications for global radar observations. *J Appl Meteorol Climatol* 51:392–404
- Lim YS, Kim JK, Kim JW, Park BI, Kim MS (2015) Analysis of the relationship between the kinetic energy and intensity of rainfall in Daejeon, Korea. *Q Int* 384:107–117
- Loh JL, Lee D-I, You C-H (2019) Inter-comparison of DSDs between Jincheon and Miryang at South Korea. *Atmos Res* 227:52–65
- Ma Y, Ni G, Chandra CV, Tian F, Chen H (2019) Statistical characteristics of raindrop size distribution during rainy seasons in the Beijing urban area and implications for radar rainfall estimation. *Hydrol Earth Syst Sci* 23:4153–4170
- Marshall JS, Palmer WM (1948) The distribution of raindrops with size. *J Meteorol* 5:165–166
- Marshall JS, Hitschfeld W, Gunn KLS (1955) Advances in radar weather. *Adv Geophys* 2:1–56
- Morrison H, Milbrandt JA (2015) Parameterization of cloud microphysics based on the prediction of bulk ice particle properties. Part I: scheme description and idealized tests. *J Atmos Sci* 72:287–311
- Murata F, Terao T, Chakravarty K, Syiemleih HJ, Cajee L (2020) Characteristics of orographic rain drop-size distribution at Cherrapunji, Northeast India. *Atmosphere* 11:777
- Niu S, Jia X, Sang J, Liu X, Lu C, Liu Y (2010) Distributions of raindrop sizes and fall velocities in a semiarid plateau climate: convective versus stratiform rains. *J Appl Meteorol Climatol* 49:632–645
- Nzeukou A, Sauvageot H, Ochou AD, Kebe CMF (2004) Raindrop size distribution and radar parameters at Cape Verde. *J Appl Meteorol* 43:90–105
- Seela BK, Janapati J, Lin P-L, Reddy KK, Shirooka R, Wang PK (2017) A comparison study of summer season raindrop size distribution between Palau and Taiwan, two islands in western Pacific. *J Geophys Res: Atmos* 122:11787–11805
- Seela BK, Janapati J, Lin PL, Wang PK, Lee MT (2018) Raindrop size distribution characteristics of summer and winter season rainfall over north Taiwan. *J Geophys Res: Atmos* 123:11–602
- Suh S-H, You C-H, Lee D-I (2016) Climatological characteristics of raindrop size distributions in Busan, Republic of Korea. *Hydrol Earth Syst Sci* 20:193–207
- Suh S-H, Kim H-J, Lee D-I, Kim T-H (2021) Geographical characteristics of raindrop size distribution in the southern parts of South Korea. *J Appl Meteorol Climatol* 60:157–169
- Testud J, Oury S, Black RA, Amayenc P, Dou X (2001) The concept of “normalized” distribution to describe raindrop spectra: a tool for cloud physics and cloud remote sensing. *J Appl Meteorol* 40:1118–1140
- Thompson EJ, Rutledge SA, Dolan B, Thurai M (2015) Drop size distributions and radar observations of convective and stratiform rain over the equatorial Indian and west Pacific Oceans. *J Atmos Sci* 72:4091–4125
- Thurai M, Gatlin PN, Bringi VN (2016) Separating stratiform and convective rain types based on the drop size distribution characteristics using 2D video disdrometer data. *Atmos Res* 169:416–423
- Tokay A, Short DA (1996) Evidence from tropical raindrop spectra of the origin of rain from stratiform versus convective clouds. *J Appl Meteorol* 35:355–371

- Tokay A, Wolff DB, Petersen WA (2014) Evaluation of the new version of the laser-optical disdrometer, OTT Parsivel<sup>2</sup>. *J Atmos Ocean Technol* 31:1276–1288
- Ulbrich CW (1983) Natural variations in the analytical form of the raindrop size distribution. *J Clim Appl Meteorol* 22:1764–1775
- Wu Z, Zhang Y, Zhang L, Lei H, Xie Y, Wen L, Yang J (2019) Characteristics of summer season raindrop size distribution in three typical regions of western Pacific. *J Geophys Res: Atmos* 124:4054–4073
- You C-H, Lee D-I (2015) Decadal variation in raindrop size distributions in Busan, Korea. *Adv Meteorol* 2015:329327
- Zea LR, Nesbitt SW, Ladino A, Hardin JC, Varble A (2021) Raindrop size spectrum in deep convective regions of the Americas. *Atmosphere* 12:979
- Zhang G, Vivekanandan J, Brandes E (2001) A method for estimating rain rate and drop size distribution from polarimetric radar measurements. *IEEE Trans Geosci Remote Sens* 39:830–841
- Zhang G, Vivekanandan J, Brandes EA, Meneghini R, Kozu T (2003) The shape–slope relation in observed gamma raindrop size distributions: Statistical error or useful information? *J Atmos Ocean Technol* 20:1106–1119
- Zhang Asi, Hu Junjun, Chen Sheng, Hu Dongming, Liang Zhenqing, Huang Chaoying, Xiao Liusi, Min Chao, Li Haowen (2019) Statistical Characteristics of Raindrop Size Distribution in the Monsoon Season Observed in Southern China. *Remote Sensing* 11(4):432. <https://doi.org/10.3390/rs11040432>

**Publisher's note** Springer Nature remains neutral with regard to jurisdictional claims in published maps and institutional affiliations.

Springer Nature or its licensor holds exclusive rights to this article under a publishing agreement with the author(s) or other rightsholder(s); author self-archiving of the accepted manuscript version of this article is solely governed by the terms of such publishing agreement and applicable law.